SANDIA REPORT
SAND2018-12313
Unlimited Release
Printed October 2018

Chemical-Mechanical Modeling of Subcritical-to-Critical Fracture in Geomaterials

Louise J. Criscenti, Jessica Rimsza, Reese E. Jones, Edward N. Matteo, Clay Payne, Adri C.T. van Duin, and Seung Ho Hahn

Prepared by
Sandia National Laboratories
Albuquerque, New Mexico 87185 and Livermore, California 94550

Sandia National Laboratories is a multi-mission laboratory managed and operated by National Technology and Engineering Solutions of Sandia, LLC, a wholly owned subsidiary of Honeywell International, Inc., for the U.S. Department of Energy's National Nuclear Security Administration under contract DE-NA0003525.

Issued by Sandia National Laboratories, operated for the United States Department of Energy by National Technology and Engineering Solutions of Sandia, LLC.

Available to DOE and DOE contractors from

U.S. Department of Energy
Office of Scientific and Technical Information
P.O. Box 62
Oak Ridge, TN 37831

Telephone: (865) 576-8401
Facsimile: (865) 576-5728
E-Mail: reports@osti.gov
Online ordering: http://www.osti.gov/scitech

Available to the public from

U.S. Department of Commerce
National Technical Information Service
5301 Shawnee Rd
Alexandria, VA 22312

Telephone: (800) 553-6847
Facsimile: (703) 605-6900
E-Mail: orders@ntis.gov
Online order: https://classic.ntis.gov/help/order-methods/

SAND2018-12313
Printed October 2018
Unlimited Release

Chemical-Mechanical Modeling of Subcritical-to-Critical Fracture in Geomaterials

Louise J. Criscenti and Jessica Rimsza
Geochemistry Department
Sandia National Laboratories
P. O. Box 5800
Albuquerque, New Mexico 87185-MS0754

Reese E. Jones
Mechanics of Materials Department
Sandia National Laboratories
P. O. Box 5800
Albuquerque, New Mexico 87185-MS9957

Edward N. Matteo and Clay Payne
Nuclear Waste Disposal Research & Analysis Department
Sandia National Laboratories
P. O. Box 5800
Albuquerque, New Mexico 87185-MS0779

Adri C.T. van Duin and Seung Ho Hahn
Pennsylvania State University
University Park, PA 16802

Abstract

Predicting chemical-mechanical fracture initiation and propagation in materials is a critical problem, with broad relevance to a host of geoscience applications including subsurface storage and waste disposal, geothermal energy development, and oil and gas extraction. In this project, we have developed molecular simulation and coarse-graining techniques to obtain an atomistic-level understanding of the chemical-mechanical mechanisms that control subcritical crack propagation in materials under tension and impact the fracture toughness. We have applied these techniques to the fracture of fused quartz in vacuum, in distilled water, and in two salt solutions - 1M NaCl, 1M NaOH - that form relatively acidic and basic solutions respectively. We have also established the capability to conduct double-compression double-cleavage experiments in an environmental chamber to observe material fracture in aqueous solution. Both simulations and experiments indicate that fractures propagate fastest in NaCl solutions, slower in distilled water, and even slower in air.

ACKNOWLEDGMENTS

This work was fully supported by the Laboratory Directed Research and Development program of Sandia National Laboratories. This paper describes objective technical results and analysis. Any subjective views or opinions that might be expressed in the paper do not necessarily represent the views of the U.S. Department of Energy or the United States Government.

TABLE OF CONTENTS

FIGURES

TABLES

EXECUTIVE SUMMARY

Predicting fracture initiation and propagation in materials is a critical yet unsolved problem crucial to assessing shale cap rocks at CO_2 sequestration sites; maximizing/controlling fracturing for gas and oil extraction; and predicting the corrosion and embrittlement of metals and ceramics. Experiments reported in the literature indicate that chemical reactions at fluid-geomaterial interfaces play a major role in subcritical crack growth by weakening the material and altering crack nucleation and growth rates. However, for example, engineering the subsurface fracture environment has been hindered by a lack of understanding of the mechanisms relating chemical environment to mechanical outcome, and a lack of capability directly linking atomistic insight to macroscopic observables.

We have developed molecular simulation and coarse-graining techniques to obtain an atomistic-level understanding of the chemical-mechanical mechanisms that control subcritical crack propagation in materials under tension and impact the fracture toughness (K_{IC}). Our approach includes the use of a reactive force field to allow bond-breaking at the crack tip, a combination of Grand Canonical Monte Carlo and Molecular Dynamics to insert water and ions into the crack, and an upscaling technique to obtain stress fields and the J-integral from the atomistic data.

We have applied these techniques to the fracture of fused quartz (amorphous silica) in vacuum, in distilled water, and in two salt solutions (1M NaCl, 1M NaOH) that form relatively acidic and basic solutions respectively. All aqueous solutions increase crack propagation and decrease the fracture toughness. The solution compositions impact surface protonation, dissolution rates, the curvature of the crack tip, as well as fracture propagation and toughness. Overall, our simulated results highlight differences in fracture mechanisms between acidic, basic, and neutral aqueous solutions.

We have also established the capability to use a small-scale experimental technique to look at fracture of material in aqueous solution. The double-compression double-cleavage method is designed to initiate a distinct preferential fracture pattern on a small cylinder of material under a compressive load in an environmental chamber. Fracture initiation and propagation are observed through a microscope. Experiments have been conducted for fused quartz in air, distilled water, and 1M NaCl. The primary effect of the various chemical environments was on the final observed crack length in the silica samples: the final crack lengths observed are shortest in ambient air, and longest in 1M NaCl. These results indicate that the Na^+ and Cl^- ions in solution enhance crack propagation in silica.

Strategically, this project positions Sandia National Laboratories at the forefront of using both molecular simulation and experiment to understand how chemistry impacts fracture initiation and growth, and therefore closer to selecting fluid compositions to control fracture initiation and growth. The capabilities and insight developed can benefit efforts to develop best practices for oil and gas production and improve the performance of sequestration. In addition, this project provides capabilities that can be used to examine stress-corrosion of numerous materials that impact nuclear waste sequestration, borehole integrity, nuclear weapon components, and other U.S. Department of Energy concerns.

NOMENCLATURE

MTI	Mechanical Technology Incorporated
LVDT	linear variable differential transformer
REAXFF	reactive force field

1 INTRODUCTION

Predicting fracture initiation, propagation, and sustainability in low permeability geomaterials (e.g. shales, clay barriers) is a critical yet unsolved problem crucial to assessing shale caprocks at CO_2 sequestration sites, and maximizing/controlling stimulated surface area and volumes available for gas and oil extraction. Experiments indicate that chemical reactions at fluid-geomaterial interfaces play a major role in subcritical crack growth by weakening the material and altering crack nucleation and growth rates [1,2]. However, engineering the subsurface fracture environment has been hindered by a lack of understanding of the mechanisms relating chemical environment to mechanical outcome, and a lack of capability directly linking atomistic insight to macroscale observables.

This research was largely motivated by the lack of fundamental knowledge regarding coupled chemical-mechanical fracture. Most crack propagation theories focus on the impact of stress and strain decoupled from chemical reactivity. Molecular studies of fracture have been typically limited to producing stress-strain curves, quantifying either the system-level stress or energy at which fracture propagation occurs. As such, these curves are neither characteristic of, nor insightful regarding fracture features local to the crack tip. In contrast, *configurational forces*, such as the J-integral [3,4], are specific to the crack in that they measure the energy available to move the crack and truly quantify fracture resistance. In the past, this continuum theory has been successfully applied to atomistic systems of metal crystals in vacuum [5-7].

Although most studies investigate crack propagation from a mechanics perspective only, it is known that chemical environment plays a significant role in fracture nucleation and growth [1]. Large-scale *in-situ* experiments emphasize the dramatic change in stress-strain behavior for material in an engineered environment [8]. The lack of understanding of the link between mechanical and chemical influences on a crack tip is largely due to the molecular-level details of localized reactions that occur at length and time-scales outside the resolution of standard experimental methods. Also, until recently, no simulation technique capable of bridging this gap existed either. However, reactive force fields such as the first-principles based reactive force field ReaxFF [9,10] are now available that can be used to start interrogating the separate and combined impacts of stress and chemical reactivity on crack tips.

Using ReaxFF [9,10], we developed methods to obtain a fundamental atomistic-level understanding of chemical-mechanical mechanisms that control subcritical crack propagation at an atomistic level. Then we used coarse-graining techniques to produce continuum-scale metrics such as the local stress fields at the crack tip and the fracture toughness for comparison with larger-scale experiments. This research leveraged Sandia's unique capabilities in using modeling and simulation to study both material strength and reactivity.

We have also incorporated an experimental approach in our research that is designed to investigate crack tip propagation at small scales for comparison with simulations. Although we were motivated by geoscience problems, the capabilities developed can also be used to investigate chemical-mechanical coupled processes leading to corrosion and embrittlement of metals and ceramics.

The next two sections provide the results of the simulation research and experimental research respectively. Because much of the simulation research has been published, Section 2 is primarily a list of publications and presentations that were presented during the course of the project that

focused on the simulation studies. The experimental design and preliminary experimental data collected during this project are described in Section 3.

2 ACCOMPLISHMENTS

This section provides the list of published materials produced from this project. Links to published journal articles, links to archival draft journal articles, and SAND numbers are provided where possible to provide the reader with access to the results of this three-year project. The published journal articles are based on the molecular simulation research performed. The experimental work was reported in some of the conference presentations listed below and is provided in full detail in Section 3. One final invited journal article will be submitted to Frontiers in Materials: Mechanics of Materials.

2.1 Published Journal Articles

Arancibia-Miranda, N., M. Escudey, R. Ramirez, R.I. Gonzalez, A.C.T. van Duin, and M. Kiwi Advancements on Synthesis of Building Block Materials: Experimental Evidence and Modelistic Interpretations of the Effect of Na and K on Imogolite Synthesis. J. Phys. Chem. C 121, 23, 12658-12668, 2017. https://pubs.acs.org/doi/abs/10.1021/acs.jpcc.6b12155 (Sandia LDRD funding acknowledgement).

Hahn, S.H., J.M. Rimsza, L.J. Criscenti, W. Sun, J. Du, T. Liang, S. Sinnott, and A.C.T. van Duin. Development of a ReaxFF Reactive Force Field for Na/Si/O/H and its application to the molecular dynamics study of sodium and proton self-diffusion and sodium cation/water interactions at the sodium silicate-water interface. *Journal of Physical Chemistry*, 2018, 10.1021/acs.jpcc.8b05852

Jones, R.E., J.M. Rimsza, and L.J. Criscenti. An atomic-scale evaluation of the fracture toughness of silica glass. *Journal of Physics-Condensed Matter*, 30 (24) 245901, 2018. https://www.ncbi.nlm.nih.gov/pubmed/29726844

Rimsza, J.M., R.E. Jones, and L.J. Criscenti. **Cover Article**. Crack propagation in silica from reactive classical molecular dynamics simulations. *Journal of the American Ceramic Society*, 101 (4), 1488-1499, 2018. https://onlinelibrary.wiley.com/doi/full/10.1111/jace.15292

Rimsza, J.M., R.E. Jones, and L.J. Criscenti. Interaction of NaOH solutions with silica surfaces. *Journal of Colloid and Interface Science*, 516, 128-137, 2018. SAND 2018-1338J. https://www.sciencedirect.com/science/article/pii/S0021979718300584

Rimsza, J.M., R.E. Jones, and L.J. Criscenti. Surface structure and stability of partially hydroxylated silica surfaces. *Langmuir*, 33 (15), 3882-3891, 2017. SAND 2017-2690J. https://pubs.acs.org/doi/abs/10.1021/acs.langmuir.7b00041

2.2 Journal Articles in Progress

Fedkin, M.V., Y.K.Shin, N. Dasgupta, J. Yeon, W. Zhang, D. van Duin, A. van Duin, K. Mori, A. Fujiwara, M. Masahiko, H. Nakamura, M. Okumura. Development of the ReaxFF methodology for electrolyte-water systems. (Sandia LDRD acknowledged for PSU funding).

Jones, R.E., W.C. Tucker, J.M. Rimsza, L.J. Criscenti. Atomic-scale interaction of a crack and an infiltrating fluid. Submitted to Chemical Physics Letters. Available at http://arxiv.org/abs/1808.07641

Rimsza, J.M., R.E. Jones, and L.J. Criscenti. Chemical effects on subcritical fracture in silica from molecular dynamics simulations. Accepted. Journal of Geophysical Research – Solid Earth.

2.3 Conference Presentations

2.3.1 2018

Criscenti, L., J. Rimsza, E.N. Matteo, C. Payne, W. Tucker, R.E. Jones. Stress-Corrosion Fracture of Silica in Aqueous Solutions. SAND2018-8483A. For *American Geophysical Union Fall Meeting*, December 2018.

Payne, C., E.N. Matteo, L. Criscenti, J. Rimsza, R.E. Jones. Chemical-mechanical effects on subcritical fracture initiation and propagation in fused quartz. SAND2018-8188A. For *American Geophysical Union Fall Meeting*, December 2018.

Criscenti, L.J., J.M. Rimsza, R.E. Jones, and E.N. Matteo. Coupled chemo-mechanical fracture of silica in aqueous solutions. SAND2018-3090A. *256th American Chemical Society Meeting, Boston, MA, August 29-23, 2018*.

Jones, R.E., L.J. Criscenti, J.M. Rimsza, and J.A. Zimmerman. Assessing the fracture strength of geological and related materials in fluid environments via an atomistically based J-integral. SAND2018-8182 C. *13th World Congress on Computational Mechanics, July 22-27, 2018*.

Rimsza, J.M., R.E. Jones, and L.J. Criscenti. Atomistic-scale evaluation of the fracture toughness of silicates in aqueous solutions. SAND 2018-5347C. *Meeting of the Glass and Optical Materials Division of the American Ceramic Society,* San Antonio, TX, May 17-20, 2018.

Criscenti, L.J., J.M. Rimsza, E.N. Matteo, and R.E. Jones. Coupled chemo-mechanical fracture in silica in aqueous solutions. SAND2018-5505C**.** *InterPore 2018*, New Orleans, May 2018.

Rimsza, J.M., R.E. Jones, and L.J. Criscenti. Atomistic-scale evaluation of the fracture toughness of silicates in aqueous solutions. SAND2018-2666C. *255th American Chemical Society Meeting,* New Orleans, March 17-20, 2018.

2.3.2 2017

Criscenti, L.J., J.M. Rimsza, E.N. Matteo, and R.E. Jones. Nanoscale stress-corrosion of geo-materials in aqueous solutions. SAND2017-13371C. *American Geophysical Union*, New Orleans, December 2017.

Criscenti, L.J., J.M. Rimsza, and R.E. Jones. Nanoscale stress-corrosion of silicate glass in aqueous solutions: Simulations and experiments. SAND2018-5356C. *12th Pacific Rim Conference on Ceramic and Glass Technology*, May 17-26, 2017.

Criscenti, L.J., T. Zeitler, M.T. Brumbach, T.M. Alam, M.A. Rodriguez, and K.G. Ewsuk. Tailored property and processing particle-filled-glass composite design and development. ***Invited*** presentation. SAND2017-5201C. *12th Pacific Rim Conference on Ceramic and Glass Technology*, May 21-26, 2017.

Rimsza, J.M., L.J. Criscenti, and R.E. Jones. Fracture toughness of silicates in aqueous electrolyte solutions. SAND2017-5349C. *Meeting of the Glass and Optical Materials Division of the American Ceramic Society*, May 2017.

Criscenti, L.J. Molecular modeling of multicomponent glass and glass surfaces for nuclear waste glass dissolution and glass-to-metal seals applications. SAND2017-3629C. *253th American Chemical Society, Symposium for Sue Brantley, Geochemistry Division Medal Recipient,* April 2-6, 2017.

Rimsza, J.M. et al. Atomistic-scale evaluation of the fracture toughness of silicates in aqueous environments. SAND2017-3291C. *253th American Chemical Society Meeting,* San Francisco, April 2-6, 2017.

Jones, R.E., L.J. Criscenti, and J.M. Rimsza. Assessing the fracture strength of geological and related materials via an atomistically based J-integral. SAND2017-2575C. The Minerals, Metals, and Materials Society (*TMS) Annual Meeting*, San Diego, February 26-March 2, 2017.

2.3.3 2016

Jones, R.E, L.J. Criscenti, and J.M. Rimsza. Assessing the fracture strength of geological and related materials via an atomistically based J-integral. SAND2016-12900C. *Annual Fall Meeting of the American Geophysical Union*, San Francisco, December 12-16, 2016.

Jones, R.E., L.J. Criscenti, and J.M. Rimsza. Assessing the fracture strength of geological and related materials via an atomistically based J-integral. SAND2016-10642C. *8th International Conference on Multiscale Materials Modeling*, *Dijon, France*, October 9-14, 2016.

Jones, R.E., L.J. Criscenti, and J.M. Rimsza. Assessing the fracture strength of geological and related materials via an atomistically based J-integral. SAND2016-8861C. *USACM: Recent Advances in Computational Methods for Nanoscale Phenomena*, Ann Arbor, MI, August 29-31, 2016.

2.4 Other Presentations

Rimsza, et al. Dissolution and fracture properties of amorphous silica through classical molecular dynamics simulations. Colorado School of Mines.

Criscenti, L.J., J.M. Rimsza, E.N. Matteo, R.E. Jones. *Nanoscale stress-corrosion of silicate glass in aqueous solutions*. SAND2017-8333C. *Invited Presentation*, BES Geosciences PI meeting, Leesburg, VA, August 7-8, 2017.

Criscenti, L.J., T. Dewers, R. Jones, S. Teich-McGoldrick, J.A. Zimmerman, and S.J. Altman. *Chemical-Mechanical Modeling of Subcritical-to-Critical Fracture in Geomaterials*. SAND2015-6850D. Geosciences Advisory Board, 2015.

Criscenti, L.J., R.E. Jones, J. M. Rimsza, E.N. Matteo, and T. Dewers. *Chemical-Mechanical Modeling of Subcritical-to-Critical Fracture in Geomaterials*. SAND2016-9669D. Poster for Sandia Geosciences Research Foundation External Advisory Board Review, October 2016.

Criscenti, L.J. et al. *Chemical-mechanical modeling of subcritical-to-critical fracture in geomaterials*. SAND2017-12571D. Poster for External Advisory Board for Geosciences Research Foundation, December 2017.

Criscenti, L.J., R.P. Muller, R.E. Jones, J.M. Rimsza, and E.N. Matteo. Chemical-mechanical modeling of subcritical-to-critical fracture in geomaterials. SAND2017-13214C. Poster for Sandia Geosciences Research Foundation external advisory board, January 2018.

Rimsza, J.M. and L.J. Criscenti. *10th Annual Postdoctoral Technical Showcase in Albuquerque, NM.* SAND2017-5271D. November 8, 2016.

Rimsza, J.M., R.E. Jones, L.J. Criscenti. Atomistic-scale evaluation of the fracture toughness of silicates in aqueous solutions. 11th *Annual Postdoctoral Technical Showcase in Albuquerque, NM.* SAND2017-11862A; SAND2017-12571D. November 21, 2017.

Rimsza, J.M., L.J. Criscenti, R.E. Jones, J. Du, J. Kelber, L. Deng, H. Kazi, F. Pasquale, A. van Duin, S. Ho, J. Yun. Dissolution and fracture properties of amorphous silica through classical molecular dynamics simulations. SAND2017-11780PE. September 22, 2017.

Rimsza, J.M., L.J. Criscenti, R.E. Jones, J. Du, J. Kelber, L. Deng, H. Kazi, F. Pasquale, A. van Duin, S. Ho, J. Yun. Dissolution and fracture of amorphous silica. Invited talk at Corning, Inc., August 14-15, 2017, NY. SAND2107-8617PE.

3 EXPERIMENTS

3.1 Methods and Materials

3.1.1 Fused Quartz Samples

Using the method developed by Celarie et al. [11, 12], fused quartz was chosen as the fracture propagation medium for this study due to its amorphous silica network and the ease with which it can be imaged via microscopy. The fused quartz specimens are rectangular prisms manufactured by Mark Optics with a length of 25 mm, width of 5 mm (Figure 3-1). Two of the 5x25 mm sides of the sample were polished to improve clarity of the crack propagation. A 1 mm diameter hole is drilled through the sample, perpendicular to the polished faces. The other sides remained unpolished with a roughness of 60/40 grit. This design was chosen to promote uniaxial crack propagation through the center of the sample.

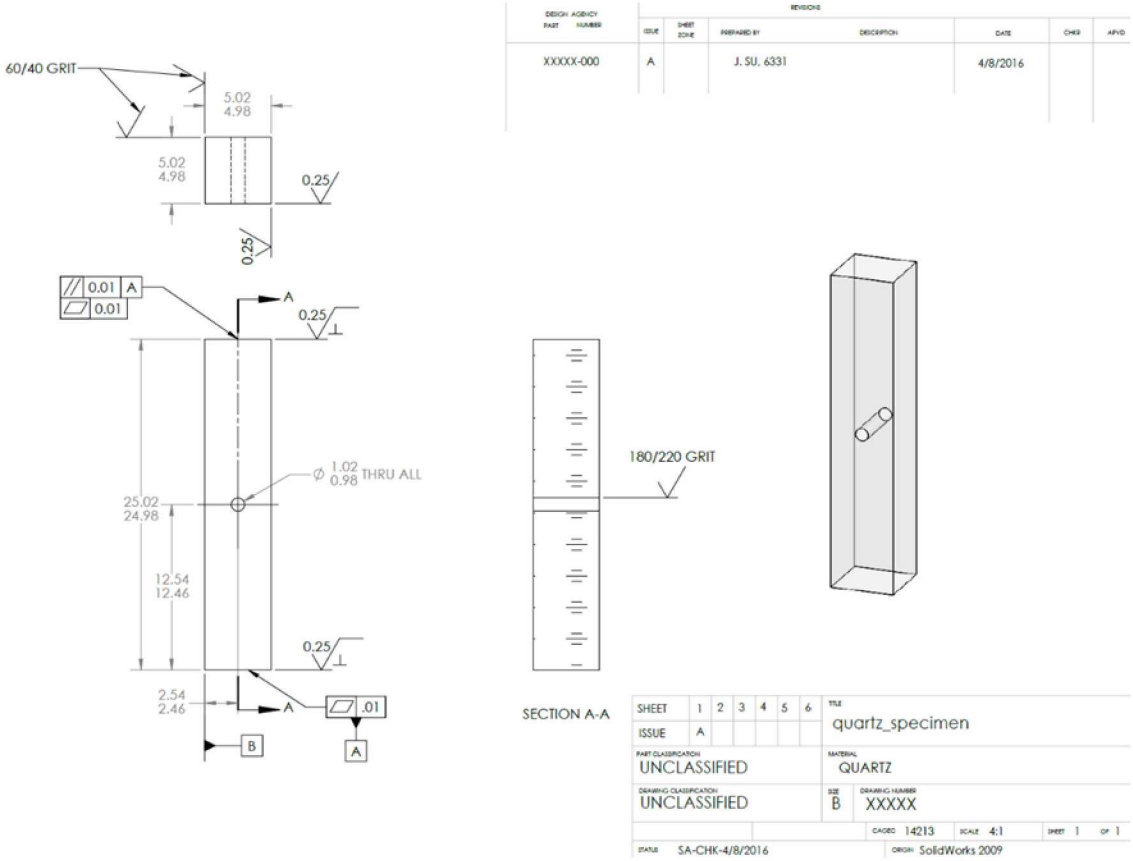

Figure 3-1. Schematic design for the fused quartz specimen.

3.1.2 Equipment

A miniature load frame (Figure 3-2) manufactured by Mechanical Technology Incorporated (MTI) Instruments was used in conjunction with MTESTQuattro software by Admet. The load frame accepts sample lengths ranging from 1 mm up to 5 cm. The frame has a maximum load of 5 kN and maximum position jog rate of 10 mm/min. MTESTQuattro is an advanced materials testing system software for servo-hydraulic and electromechanical testing machines [13]. Crack propagation was observed by using a Zeiss Stemi SV11/stereomicroscope paired with an

Axiocam 105C microscope camera (Figure 3-3). The camera captured a 7 x 9.5 mm rectangular area at a magnification of 6x. The optics system was controlled using Zeiss Zen software with the time lapse module. All software was consolidated on one laptop, which allows for greater mobility of the system if desired.

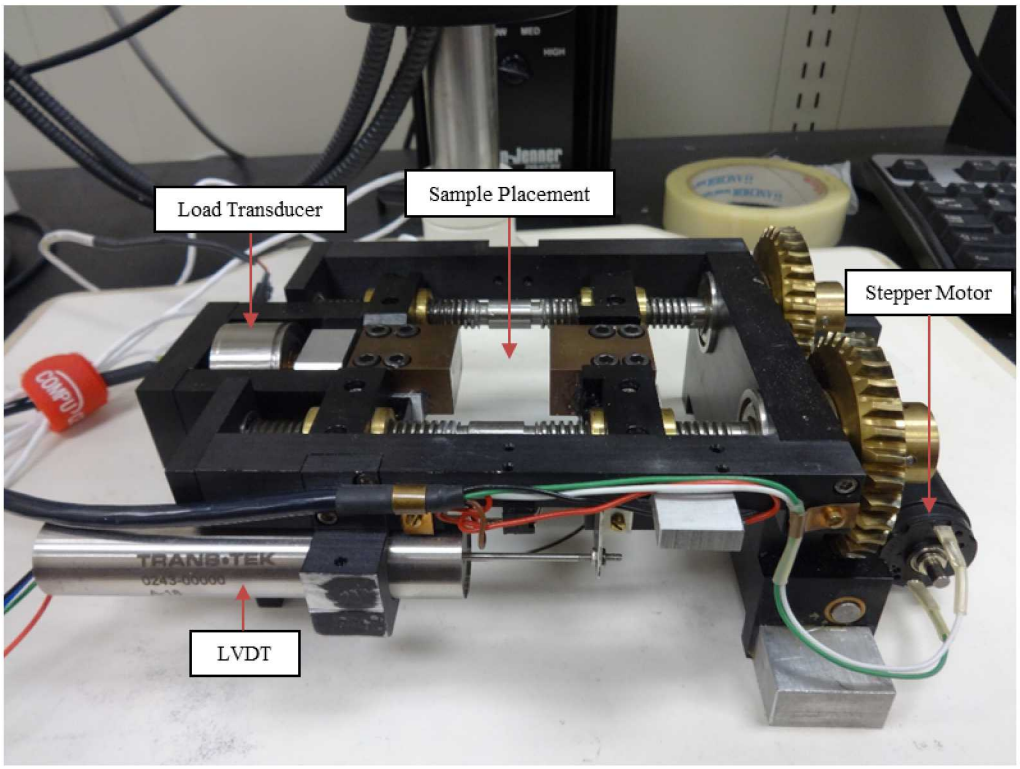

Figure 3-2. MTI Instruments load frame with major components identified.

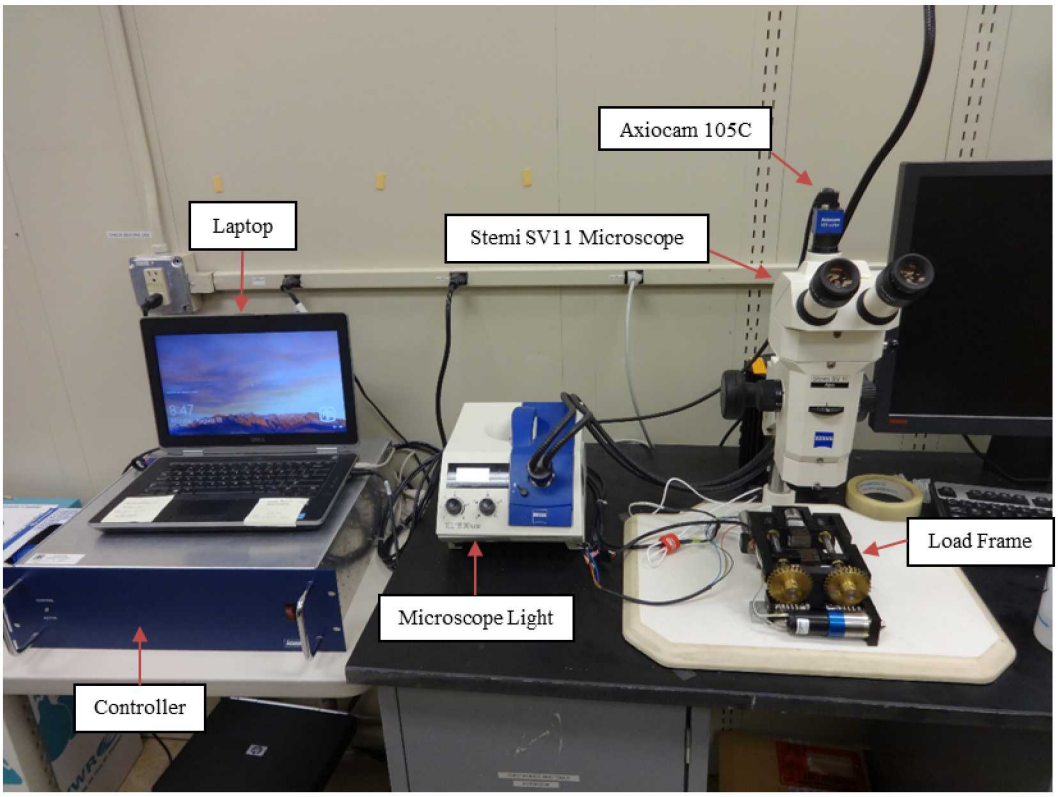

Figure 3-3. Experimental setup including: load frame, microscope, camera, microscope light, controller, and laptop.

3.1.3 Compression Procedure

The compression procedure consisted of two test sequences controlled by the MTESTQuattro software: 1) compression to crack initiation, and 2) subcritical crack growth at a constant displacement. Each sample was subjected to both test sequences, the use of two test sequences was necessitated by the constraints of the control software. In effect, the tests sequences compromise a single test, with two sub-tests. The fused quartz sample is placed into the load frame, and held in place by compression until the sample was seated in the load frame (<10 N for static hold). Clear Teflon sheets were used as flats on either side of the specimen, to avoid point-loading on the ends of the sample during alignment/loading of the sample. After testing other metallic foils as compression flats, Teflon was selected both for its relatively low mechanical compliance, as well as for its chemical inertness in the submersed tests. After the sample was inserted in the load frame, the initial load program and time lapse programs were started. The initial load program was performed by implementing a constant ramp rate of 0.05 mm/min on the sample while taking 100 samples/sec. The test continued until an initial fracture was observed through the central void of the sample. Upon observing the initial fracture (Figure 3-4) the load frame was held at a constant position and the load relaxation program was started. The load relaxation program monitored the load on the sample when held at a constant position. This resulted in the observation of the load relaxation as function of crack displacement in the fused quartz samples. All samples were examined for 24 hours to monitor the load relaxation.

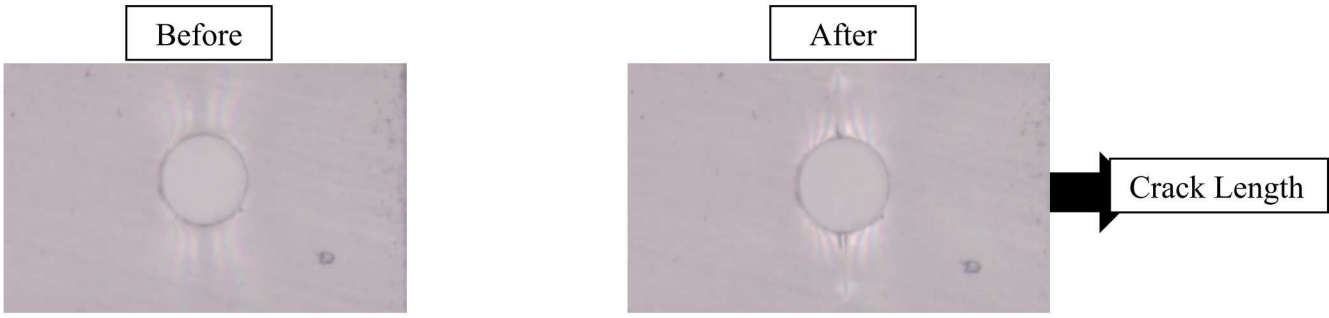

Figure 3-4. Photographs depicting the sample before crack initiation followed by a photograph just after initial crack formation.

3.1.4 Chemical Environmental Chamber

The chemical environmental chamber was made by forming an open rectangular box using clear Teflon sheets (Figure 3-5). The rectangular box had a length of 2.5 cm, width of 2 cm and a height of 2 cm. The fused quartz samples were placed below the water line in the rectangular box so as to remain submerged for the duration of the test. The three chemical environments that were examined were ambient air, de-ionized water, and 1M NaCl.

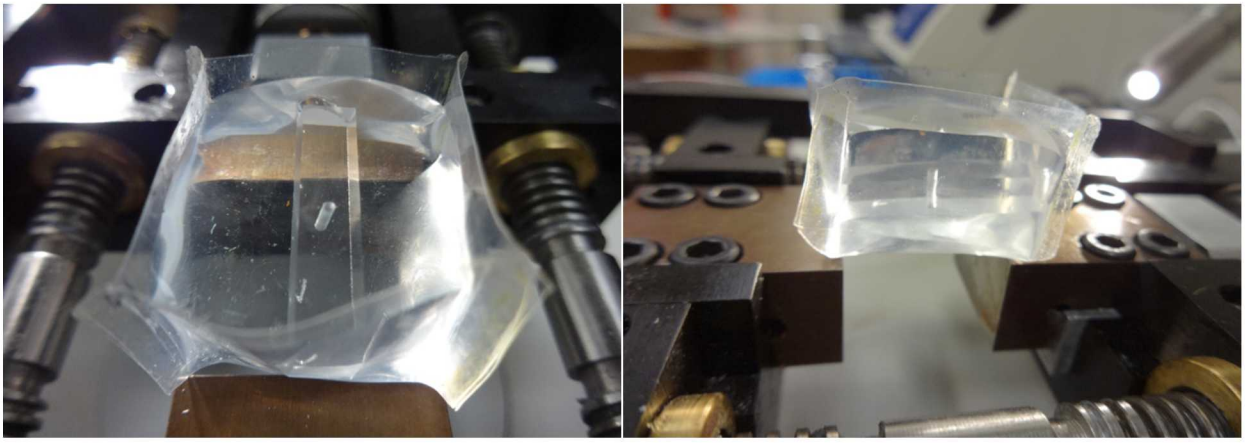

Figure 3-5. Chemical environment chamber, shown holding sample in de-ionized water.

3.1.5 Systems Upgrades/troubleshooting

The load frame system had outdated software and hardware components, therefore, and as the system was tested for repeatability, it became necessary to upgrade components of the testbed. The first software component that was replaced was the older version of the MTESTQuattro software (v 2.01.01). The newest version of the software was purchased (v 5.07.02), which allowed the continuous monitoring of the load at a constant position. The newer software version also provided the capability to measure certain material properties directly within the program. Updated software for the microscope camera was also obtained. The software was updated from AxioVison 4.4 to Zen software by Zeiss. The Zen software includes a time lapse module that allows continuous photo capturing of the crack propagation.

New hardware improvements were also made, in order to enhance the capabilities of the system. The first hardware purchase was a new microscope camera, the Axiocam 105C. The Axiocam

105C has an exposure time of 100 µs to 2 s and a live frame rate of up to 47 fps. The camera is connected via USB 3.0 cable which allows high speed data transfer and the ability to acquire color images with 5 megapixels [14]. The next piece of hardware that was purchased for the system was a new linear variable differential transformer (LVDT). The LVDT is an electromechanical transducer that can convert the rectilinear motion of an object to which it is coupled mechanically into a corresponding electrical signal [15]. The final piece of hardware that was added to the system was the updated laptop. The laptop replaced a much older desktop which allowed the new software to run seamlessly. The incorporation of a laptop also added mobility to the system so that the load frame can be moved to accommodate a variety of testing envelopes.

3.2 Results and Discussion

Compression tests were conducted in triplicate in Air, de-ionized water, and 1M NaCl. Since the system is capable of measuring and recording load, displacement, and time, there are several options for post-test data analyses. The data are presented in three was: 1) Crack length vs. time, 2) Load vs. Position, and 3) Load vs. Time. The results from each chemical environment (air, water, 1M NaCl) are discussed separately in Sections 3.2.1, 3.2.2, and 3.2.3. Comparisons are made between the chemical environments to assess potential chemo-mechanical effects of chemical environment on fracture propagation.

3.2.1 Fracture Propagation in Air

Three separate compression tests were performed on the fused quartz specimens in ambient air. The results of the fracture propagation over the 24 hour period is shown below in Figure 3-6.

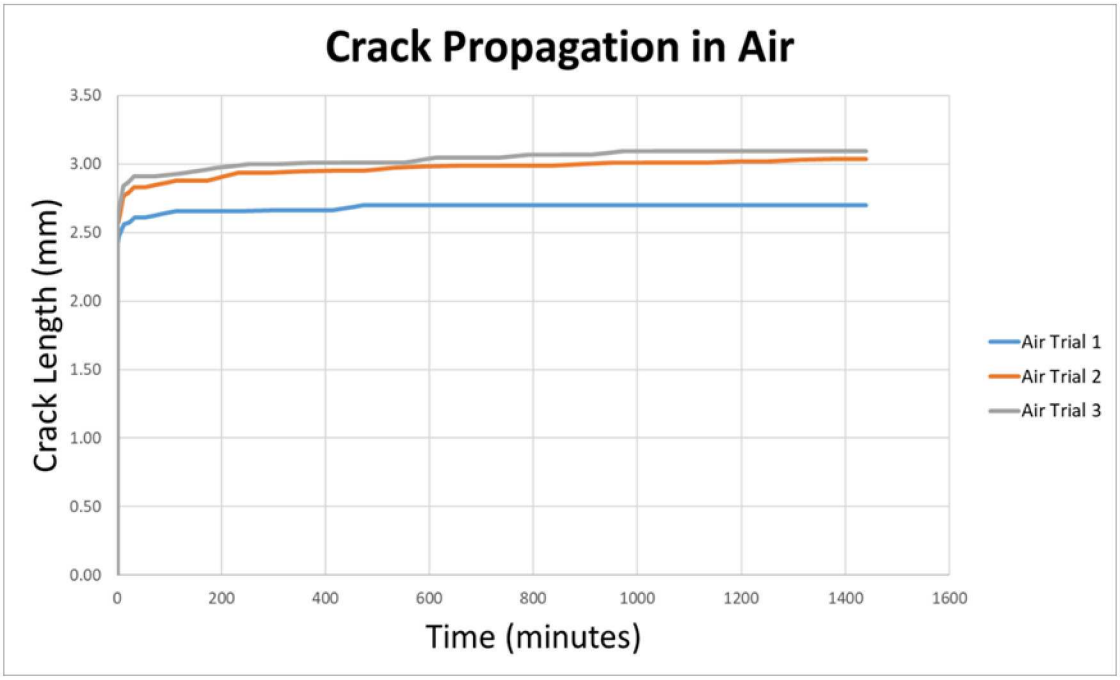

Figure 3-6. Crack length propagation observed in ambient air over a 24 hr observation period.

The average initial crack length observed in the quartz samples in ambient air was 1.42 ± 0.6 mm with an average final crack length of 2.94 ± 0.2 mm. As observed in Figure 3-6. the crack length grows rapidly upon the initial fracture, but then slows substantially. The quartz samples in ambient air reached an average of 86% of the final crack length within the first 60 seconds of fracture initiation. The fracture then propagated the remaining 14% over 24 hours.

The load required to initiate fracture in the quartz samples in ambient air was then examined. The results are summarized below in Figure 3-7.

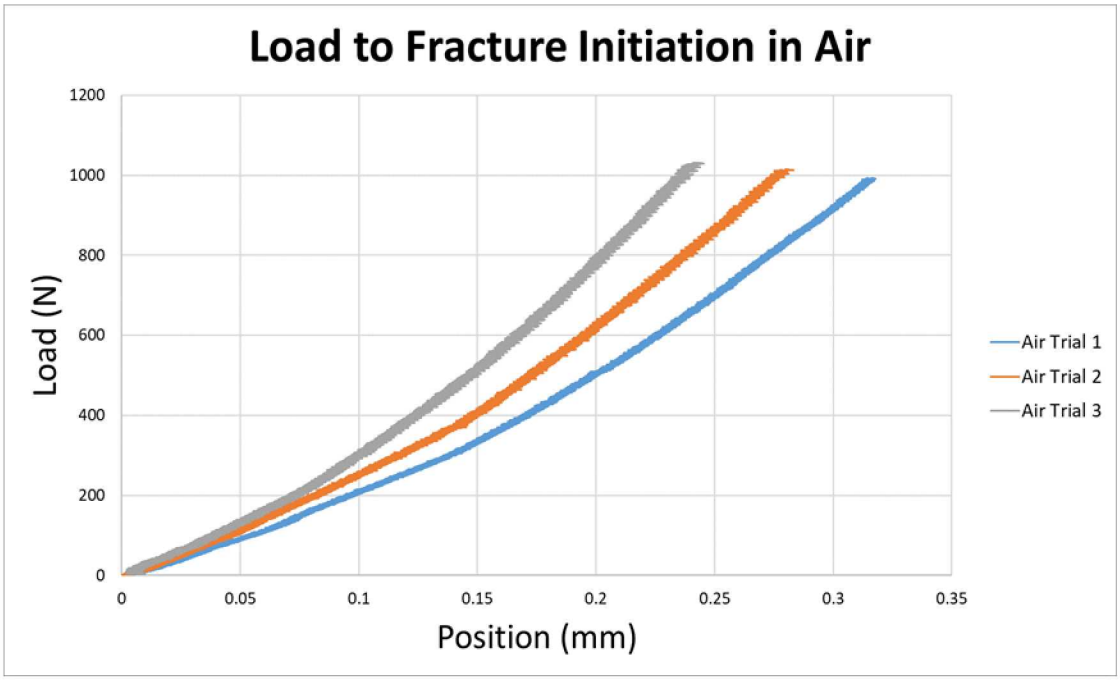

Figure 3-7. Load versus position and the load required to initiate fracture in the quartz specimens in ambient air

The average load required for fracture initiation in ambient air was 1011 ± 15 N. The load required to initiate fracture varies only ~15 N between samples which demonstrates consistency of fracture behavior in ambient air. Figure 3-7 illustrates the load versus position for the fused quartz in ambient air. There is a variance in the position at which the initial fracture occurs, this can perhaps be attributed to the seating of the sample, although results for the other two chemical environments may also suggest another cause for this position variance, such as localized chemical environment at the crack tip. Unlike the Air case, the water case (see next section), shows very little variance for the load vs. position plot, in fact, the curves lie on top of one another. For the air case, there are two apparent phases in which the slope of the curves change. In the first phase (0-0.2mm) each of the samples have a slightly different slope due to the seating of the samples. The plots demonstrate similar slopes for the final 500 N of the load. This is demonstrated below in Figure 3-8.

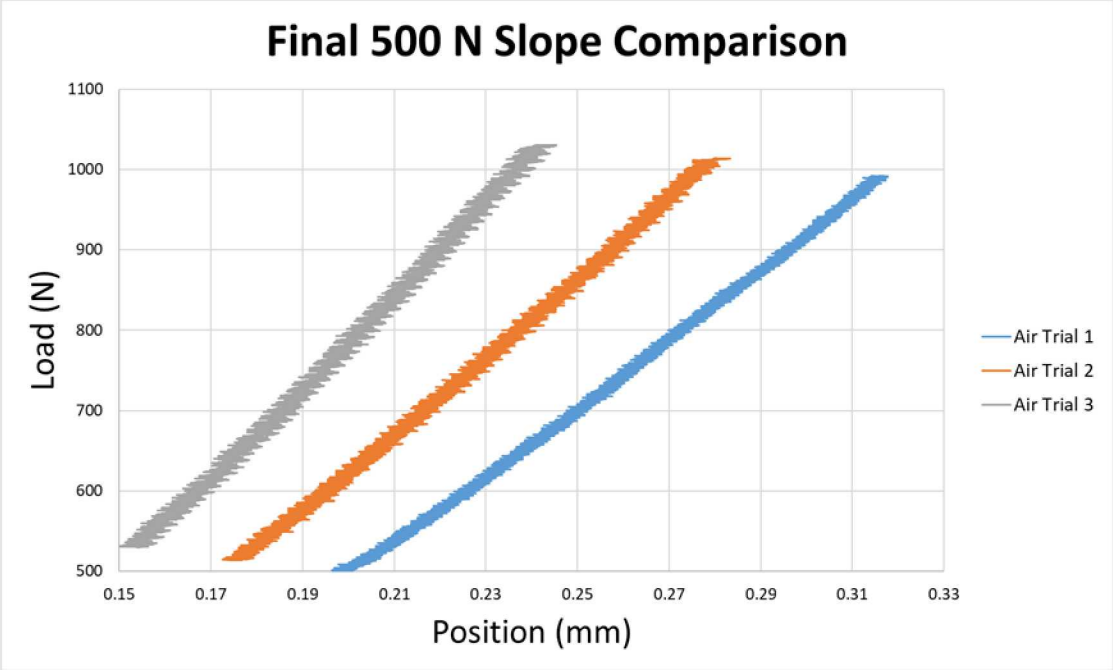

Figure 3-8. Load vs Position for final 500N of load on fused quartz speciments in air.

The final fracture property observed was the load relaxation of the quartz samples as a function of time. In theory, as the crack propagates there will be a decrease in the load on the sample due to the stress relaxation associated with crack propagation. The results of the change in load as a function of time are shown below in Figure 3-9.

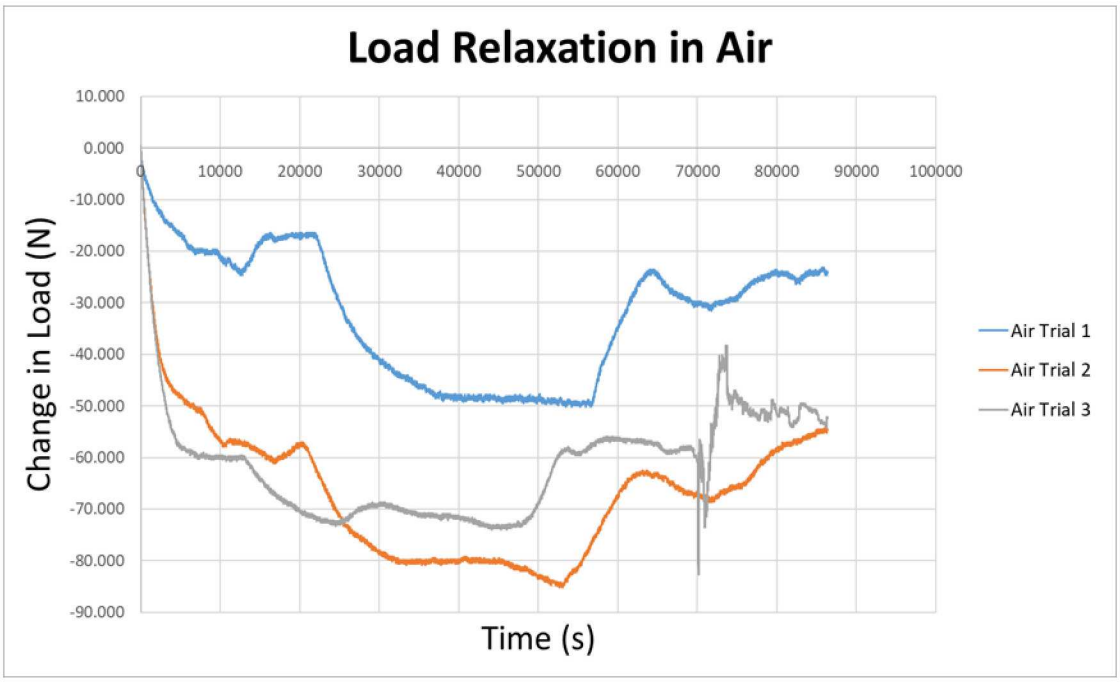

Figure 3-9. Load relaxation of the quartz samples in ambient air versus time.

The load relaxation in the samples shows a general trend of decreasing as a function of time, which represents the load relaxation expected to occur the fracture provides stress relief to the sample. The plots demonstrate similar trends between samples upon which a change in load decreases rapidly, remains constant, or in some cases even increases slightly. There is a curious uptick in load (~25N) at long times, which could be attributable to controller drift or perhaps some as of yet understood phenomenon occurring in the glass samples. Further tests, including control samples, would need to be conducted to ascertain the nature of this uptick in load.

3.2.2 Fracture Propagation in De-Ionized Water

Triplicate compression tests were performed on the fused quartz specimens in de-ionized water. The results of the fracture propagation over a 24 hour period are shown below in Figure 3-10.

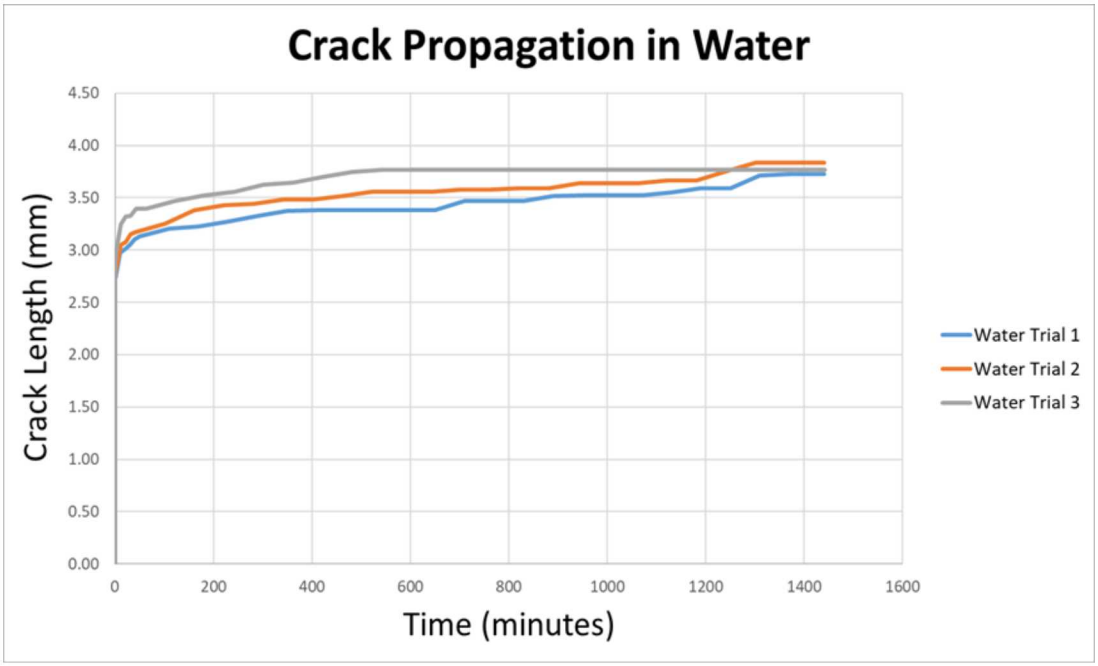

Figure 3-10. Crack propagation in de-ionized water over a 24 hour period.

The average initial fracture length in the fused quartz samples in de-ionized (DI) water was 2.02 ± 0.7 mm with an average final crack length of 3.77 ± 0.04 mm. The final crack length at the 24 hour mark demonstrated very little variation between samples with a deviation of only 0.04 mm between samples. The quartz samples in DI water reached an average of 75% of the overall crack length propagation within the first 60 seconds of fracture initiation.

The load versus position data as well as the load at which the initial fracture occurred was then examined for the quartz samples in DI water. The results are shown below in Figure 3-11.

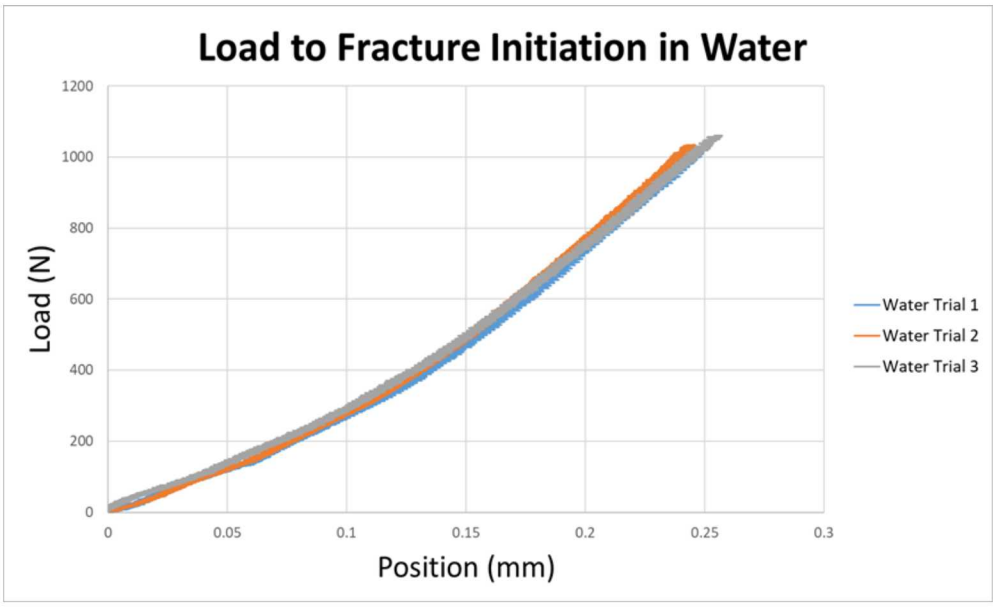

Figure 3-11. Load versus position data as well as load at fracture initiation for the fused quartz samples in DI water.

The average load required for fracture initiation in DI water was 1040 ± 14 N. There is little variation observed between samples for the load required to initiate fracture, 14 N. The plots for all three of the trials are very similar. It seems as though the samples are seated in a more consistently when submersed in water, and therefore, the load versus position data shows greater repeatability

The load relaxation of the quartz sample as a function of time and crack propagation was then observed. The results are shown in Figure 3-12.

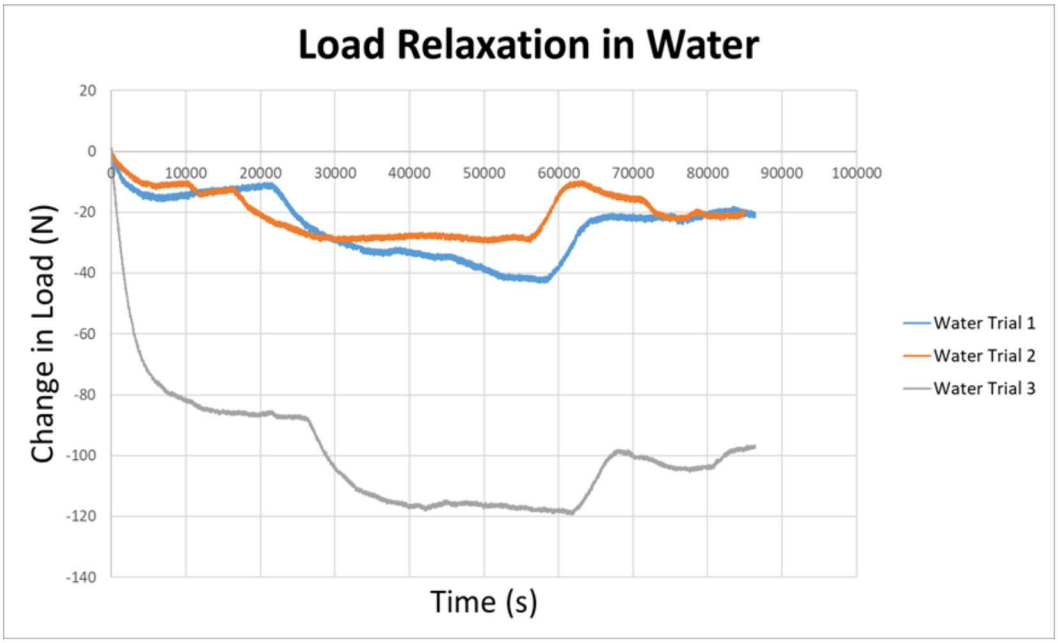

Figure 3-12. Load relaxation in the fused quartz samples as a function of time and crack propagation.

The three load relaxation plots in DI water show similar trends between trials. There is a rapid decrease in load upon the initial fracture occurring followed by a relatively constant phase and finally ended with a slight increase in load before the load steadies again. Trial 3 demonstrates a much larger change load than trial 1 and 2. However, the overall crack length in trial 3 is slightly less than the overall crack length in trial 2. Therefore, for the fracture propagation in water there does not seem to be a strong correlation between the maximum change in load and overall crack propagation.

3.2.3 Fracture Propagation in 1M Sodium Chloride (NaCl)

Three replicate compression tests were performed on the fused quartz specimens in a 1M NaCl solution. The fracture propagation over a 24 hour period in 1M NaCl is shown below in Figure 3-13.

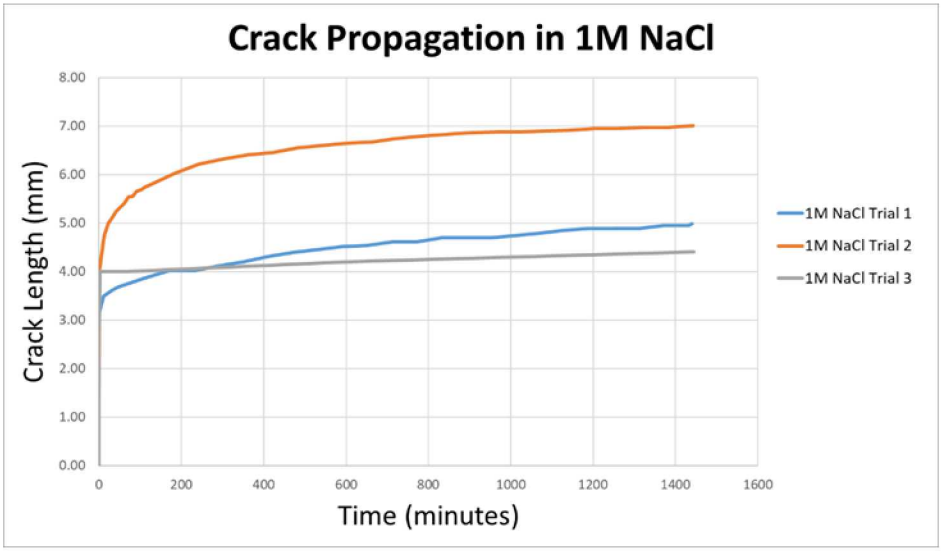

Figure 3-13. Fracture propagation as a function of time in 1M NaCl.

The average initial crack length for the fused quartz in 1M NaCl was 2.35 ± 0.7 mm with an average final crack length of 5.47 ± 1 mm. The final crack length at the end of the 24 hour period demonstrated a larger variance between samples than observed in water and ambient air. The increase in variance for the final crack length can be attributed to the continued crack propagation as a function of time. The fused quartz samples reached an average of 62% of the final crack length within 60 seconds of fracture initiation.

The load at which fracture initiation occurred was then examined for the fused quartz samples in 1M NaCl. The results are shown in Figure 3-14.

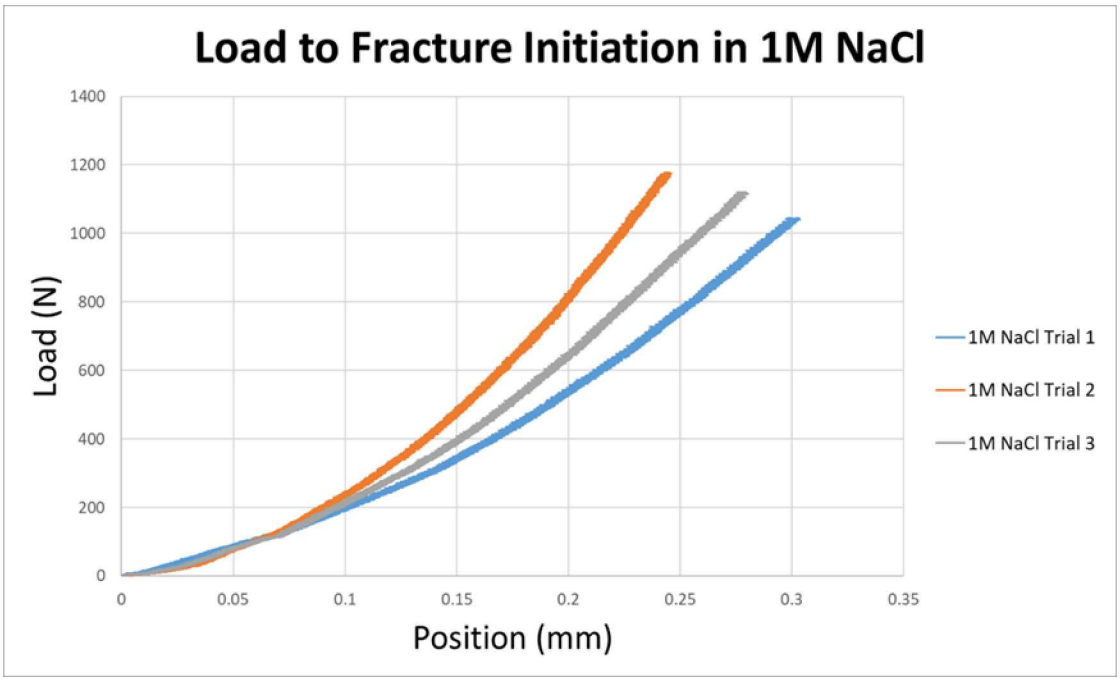

Figure 3-14. Load versus position and load at which fracture occurs for fused quartz in 1M NaCl.

The average load required for fracture initiation in 1M NaCl was observed to be 1113 ± 54 N. The average magnitude of the load required to initiate fracture is higher in 1M NaCl than the other two environments. There is also a larger variance between samples in the required load for fracture initiation, as was seen in the tests in Air (see Section 3.1.1). The samples in 1M NaCl demonstrate similar trends during the early load stages, but as the load increases the variance in the plots also increases. The slopes of the curves after ~0.1mm on the position axis seem to differ slightly between samples. This observation indicates that the NaCl in solution is altering the mechanical properties of the quartz specimens and thus leads to a greater variance between samples.

The load relaxation of the quartz samples in 1M NaCl was then examined. The results are shown in Figure 3-15. The load relaxation curves in 1M NaCl demonstrate similar trends as observed in the load relaxation data in DI water and ambient air. Trial 1 in NaCl demonstrates the largest decrease in load as a function of time as compared to trial 2 and 3. However, as was observed in the DI water, the total crack length in Trial 1 is less than the total crack length observed in Trial 2. This observation indicates that there is not a strong correlation between load relaxation and final crack length in 1M NaCl.

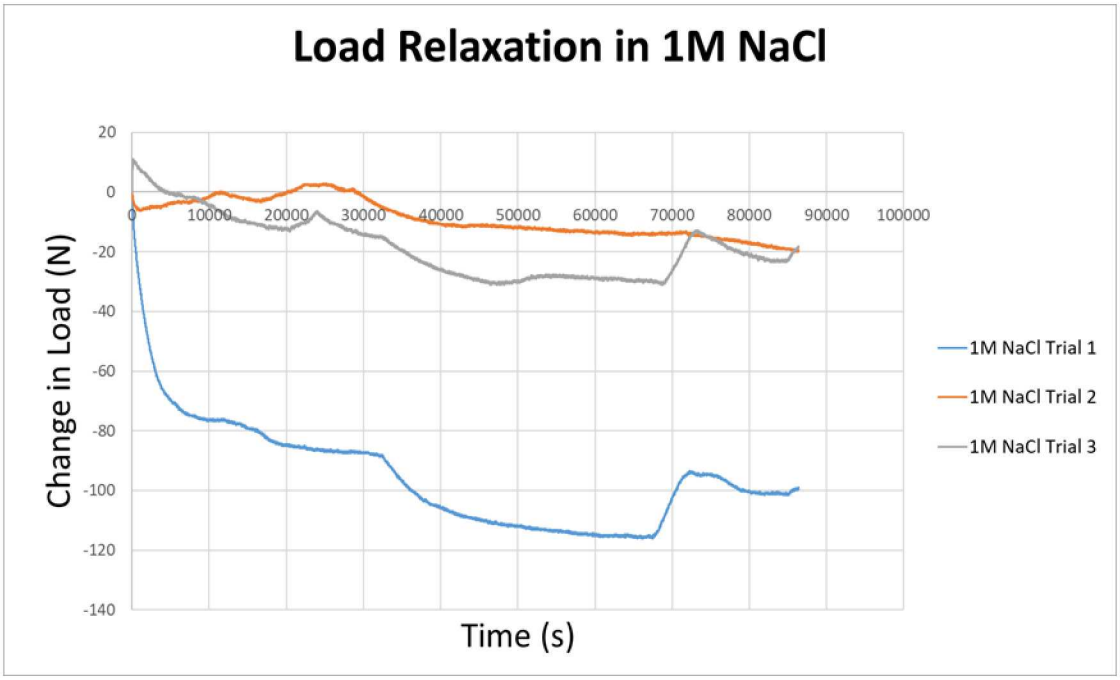

Figure 3-15. Change in load versus time for fused quartz in 1M NaCl.

3.3 Summary

The fracture behavior of fused quartz samples were examined in three chemical environments: ambient air, DI water, and 1M NaCl. The results indicate that the chemical environment has an effect on the fracture behavior in the fused quartz specimens. The primary effect the various chemical environments was on the final observed crack length in the specimens after 24 hours of crack propagation. A summary of those results is shown in Figure 3-16. It is observed that the lowest average final crack length is observed in the quartz samples in ambient air, followed by DI water and finally the maximum final crack propagation is observed for the samples in 1M NaCl. These results indicate that the Na^+ and Cl^- ions in solution enhance crack propagation in the fused quartz. Future work should include further testing to discern if the load increase at long times is related to test rig control issues, or otherwise if some phenomenon within the samples could reverse the load relaxation seen as the crack propagates.

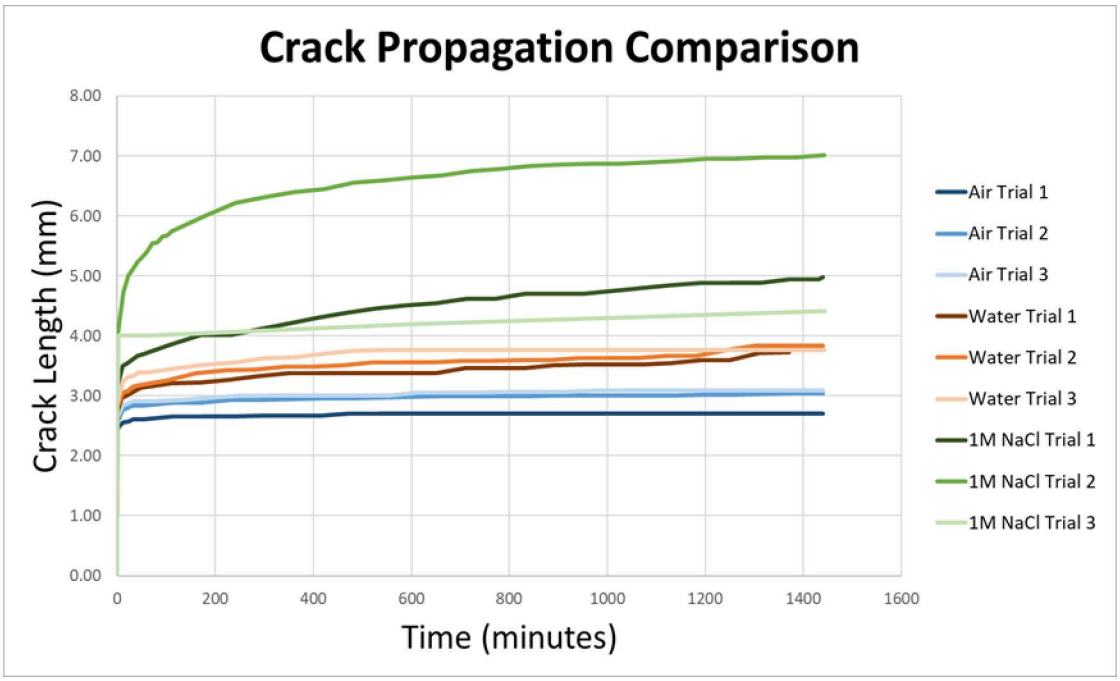

Figure 3-16. Crack propagation comparison of all the samples in the different chemical environments.

The chemical environment also had an effect on other fracture properties observed as well as the final crack length. The observed results are shown in Table 3-1.

Table 3-1. Summary of the average fracture properties observed in the three chemical environments

Chemical Environment	Initial Crack Length (mm)	Final Crack Length (mm)	% of total Crack Length @(60 sec)	Peak Load (N)
Ambient Air	1.42 ± 0.6	2.94 ± 0.2	86%	1011 ± 15
DI Water	2.02 ± 0.7	3.77 ± 0.04	75%	1040 ± 14
1M NaCl	2.35 ± 0.7	5.47 ± 1	62%	1113 ± 54

As you move from ambient air to NaCl in the Table 3-1 we see an increase in the initial crack length formed upon initial fracture. We also see the same trend in the final crack length observed; the shortest average final crack length is found in the samples in ambient air and the longest final crack length was found in the 1M NaCl chemical environment.

The average peak load required to initiate fracture increases as you move from ambient air to 1M NaCl. This, in turn, contributes to the increase of initial crack length observed. As the peak load increases, the initial crack length also increases. One important observation found is the percentage of total crack length at 60 seconds (60 seconds was chosen as arbitrary time segment for comparison). This percentage demonstrates the crack propagation in a mechanically static state. The load frame remained at a constant position as the crack propagated through the samples. The samples in Air reached 86% of the final crack length within the first 60 seconds of

fracture initiation. The samples in DI water reached 75% of the final crack length in the first 60 seconds of fracture initiation. The samples in 1M NaCl reached 62% of the final crack length within the first 60 seconds of the fracture initiation. These results indicate that the chemical environment with the highest fracture percentage at 60 seconds had the lowest effect on the crack propagation in static conditions. The fracture percentage at 60 seconds in 1M NaCl was the lowest out of the three chemical environments tested, this in turn indicates that overall the NaCl environment increased the crack growth rate in the fused quartz samples as compared to ambient air and DI water.

In conclusion, it is apparent that the chemical environment affected the fracture propagation in the fused quartz samples. The quartz samples compressed in ambient air were treated as a base case for this experiment. DI water and 1M NaCl were then examined to determine if the incorporation of an aqueous solution had an effect on the fracture propagation. The results indicate that a quartz sample submersed in DI water demonstrates increased fracture propagation as compared to ambient air. The results also indicate that the 1M NaCl chemical environment demonstrates increased fracture propagation as compared to ambient air and DI water. Thus, a final conclusion is that of the three cases tested(Air, DI, 1M NaCl), the fracture propagation in a fused quartz sample is maximized when submersed in 1M NaCl.

4 CONCLUSIONS

Predicting fracture initiation and propagation in materials is a critical problem crucial to assessing shale cap rocks at CO_2 sequestration sites; maximizing/controlling fracturing for gas and oil extraction; and predicting the corrosion and embrittlement of metals and ceramics. Experiments reported in the literature indicate that chemical reactions at fluid-geomaterial interfaces play a major role in subcritical crack growth by weakening the material and altering crack nucleation and growth rates. However, there is a lack of understanding of the mechanisms relating chemical environment to mechanical outcome and a lack of capability directly linking atomistic insight to macroscopic observables.

We have developed molecular simulation and coarse-graining techniques to obtain an atomistic-level understanding of the chemical-mechanical mechanisms that control subcritical crack propagation in materials under tension and impact the fracture toughness (K_{IC}). Our approach includes the use of a reactive force field (ReaxFF) to allow bond-breaking at the crack tip, a combination of Grand Canonical Monte Carlo and molecular dynamics to insert water and ions into the crack, and an upscaling technique to obtain stress fields and the J-integral from the atomistic data.

We have applied these techniques to the fracture of fused quartz (amorphous silica) in vacuum, in distilled water, and in two salt solutions (1M NaCl, 1M NaOH) that form relatively acidic and basic solutions respectively. Because fracture toughness is dependent on surface energy, we first investigated the surface structure and energy as a function of silica surface hydroxylation using two force fields, ClayFF [16] and ReaxFF [10]. The ClayFF force field better matched experimental results for the energies of unhydroxylated silica fracture surfaces while the ReaxFF did a better job of matching experimental data for hydroxylated surfaces [17]. Our follow-on fracture simulations were performed with ReaxFF because we are interested in calculated surface energies in aqueous solution and because ReaxFF is a reactive force field that allows for bond-breaking and bond-making – an important feature for simulating fracture.

Next, we introduced a slit crack into an atomistic amorphous silica model and mode I stress was applied through far-field loading until the crack propagates. Atomic displacements and forces and an Irving-Kirkwood method with a Langragian kernel estimator were used to calculate the J-integral of classical fracture mechanics around the crack tip. The resulting fracture toughness (K_{IC}) agrees with experimental values. In addition, the stress fields and dissipation energies around the slit crack indicate the development of an inelastic region ~30Å in diameter [18].

To investigate changes in fracture propagation and toughness with water, we simulated (1) silica fracture in vacuum with dynamic loading, (2) an aqueous environment with dynamic loading, and (c) an aqueous environment with static subcritical mechanical loading to track silica dissolution. The addition of water to silica fracture reduced the calculated fracture toughness by ~25%, consistent with experimentally reported results. Analysis of Si-O bonds in the process zone and calculations of dissipation energy associated with fracture indicated that water relaxes the entire process zone, and not just the surface. Additionally, the crack tip sharpens during fracture in aqueous conditions and an increased number of microscopic propagation events occur. This results in earlier fracture in systems with increasing mechanical loading in aqueous solutions, despite the lack of significant silica dissolution. Therefore, the threshold for Si-O bond breakage has been lowered in the presence of water and the reduction in fracture toughness is due to structural and energetic changes in silica, rather than specific dissolution events [19].

Finally, molecular dynamics simulations have been performed for silica in 1.0M NaCl and 1.0M NaOH solutions. The addition of electrolytes results in two distinct responses in the silica. The basic solution leads to higher surface deprotonation, less dissolution, a narrower radius of curvature at the crack tip, and greater decrease in fracture toughness, compared to the more acidic environment. The different results in the two electrolyte solutions explain experimental observations and provides insight into how anions alter the chemical-mechanical fracture of silica.

REFERENCES

1. Dove, P.M. 1995. "Geochemical controls on the kinetics of quartz fracture at subcritical tensile stresses," *Journal of Geophysical Research*, **100**, 22349-22359.
2. Rinehart, A.J., J.E. Bishop, T. Dewers. 2015. "Fracture Propagation in Indiana Limestone Interpreted via Linear Softening Cohesive Fracture Model", *Journal of Geophysical Research – Solid Earth*, **120**, 2292-2308.
3. Eshelby, J.D. 1951. "The Force on an Elastic Singularity," Phil. Trans. Roy. Soc. London Series A: Math. Phys. Sci.
4. Rice, J.R. 1968. "A Path Independent Integral and the Approximate Analysis of Strain Concentration by Notches and Cracks", J. Appl. Mech.
5. R.E. Jones, J.A. Zimmerman. *The construction and application of an atomistic J-integral via Hardy estimates of continuum fields*. J. Mech. Phys. Solids, 2010
6. R.E. Jones, J.A. Zimmerman, J. Oswald, and T. Belytschko. *An atomistic J- integral at finite temperature based on Hardy estimates of continuum fields*, J.Phys-Cond.Mat., 2010
7. J.A. Zimmerman, R.E. Jones. *The application of an atomistic J-integral to a ductile crack*. J.Phys., 2013
8. D. White, R. Liu, B. Ganis, T. Dewers, MF. Wheeler, *Coupled Compositional Geomechanical Plasticity Models for the Cranfield Dataset*, 2015
9. van Duin, A.C.T., A. Strachan, S. Stewman, Q. Zhang, X. Xu, Xin, and W. Goddard. 2003. "ReaxFF SiO reactive force field for silicon and silicon oxide systems," Journal of Physical Chemistry A, **107**, 3803-3811.
10. Yeon, J, and A.C. T. van Duin. 2015. "ReaxFF Molecular Dynamics Simulations of Hydroxylation Kinetics for Amorphous and Nano-Silica Structure, and Its Relations with Atomic Strain Energy," *The Journal of Physical Chemistry C*, **120**, 305-317.
11. Celarie, F., M. Ciccotti, and C. Marliere. 2007. "Stress-enhanced ion diffusion at the vicinity of a crack tip as evidenced by atomic force microscopy in silicate glasses," *Journal of Non-Crystalline Solids*, **353**, 51-68.
12. Celarie, F., S. Prades, D. Bonamy, A. Dickele, E. Bouchaud, C. Guillot, and C. Marliere. 2003. "Surface fracture of glassy materials as detected by real-time atomic force microscopy (AFM) experiments," *Applied Surface Science*, **212**, 92-96.
13. MTESTQuattro. www.admet.com/products/controllers-and-indicators/mtestquattro/.
14. Axiocam 105 Color. Why Good Vision Is So Important | ZEISS United States, www.zeiss.com/microscopy/int/products/microscope-cameras/axiocam-105-color.html.
15. Basics of LVDT." Build Drones That Can Do the Impossible," www.te.com/usa-en/industries/sensor-solutions/insights/lvdt-tutorial.html. July 2017.
16. Cygan, R.T., J.-J. Liang and A.G. Kalinichev. 2004. "Molecular Models of Hydroxide, Oxyhydroxide, and Clay Phases and the Development of a General Forcefield," *Journal of Physical Chemistry B*, **108**, 1255-1266.

17. Rimsza, J.M., R.E. Jones and L.J. Criscenti. 2017. “Surface structure and stability of partially hydroxylated silica surfaces,” *Langmuir*, 10.1021/acs.langmuir.7b00041.

18. Rimsza, J.M., R.E. Jones, and L.J. Criscenti. 2018. “Crack propagation in silica from reactive classical molecular dynamics simulations,” *Journal of the American Ceramic Society* **101**, 1488-1499.

19. Rimsza, J.M., R.E. Jones, and L.J. Criscenti. (accepted) Chemical effects on subcritical fracture in silica from molecular dynamics simulations. Journal of Geophysical Research – Solid Earth.

DISTRIBUTION

2 Adri C.T. van Duin and Seung Ho Hahn
Pennsylvania State University
Department of Mechanical and Nuclear Engineering
240 Research East Building
University Park, PA 16802

1	MS0404	Stephanie Teich-McGoldrick	Org. 06752
1	MS0472	Amy Cha-Tien Sun	Org. 02334
1	MS0721	Carol L. Jones-Adkins	Org. 08800
1	MS0721	Susan J. Altman	Org. 08801
1	MS0735	Moo Y. Lee	Org. 08864
1	MS0735	Erik K. Webb	Org. 08860
1	MS0736	Patrick V. Brady	Org. 08840
1	MS0747	Robert J. MacKinnon	Org. 08844
1	MS0750	Nancy S. Brodsky	Org. 08865
1	MS0750	Jason E. Heath	Org. 08864
1	MS0750	Tracy Woolever	Org. 08162
1	MS0779	Thomas Dewers	Org. 08842
1	MS0754	Anastasia G. Ilgen	Org. 08865
1	MS0779	Kevin A. McMahon	Org. 08842
1	MS0779	Yifeng Wang	Org. 08842
1	MS0889	Michael E. Chandross	Org. 01864
1	MS0889	E. John Schindelholz	Org. 01852
1	MS0889	Kevin Strong	Org. 01851
1	MS0889	Mark Wilson	Org. 01864
1	MS1168	Thomas E. Buchheit	Org. 01356
1	MS1322	Aidan P. Thompson	Org. 01444
1	MS1411	Richard P. Muller	Org. 01864
1	MS1415	Kevin Leung	Org. 01864
1	MS1321	Veena Tikari	Org. 01444
1	MS1349	C. Jeff Brinker	Org. 01000
1	MS1415	Tina M. Nenoff	Org. 01800
1	MS1421	Jeffrey S. Nelson	Org. 01870
1	MS9042	Scott T. Peterson	Org. 08343
1	MS9054	Sarah W. Allendorf	Org. 08350
1	MS9161	Jonathan A. Zimmerman	Org. 08367
1	MS1315	Katherine L. Jungjohann	Org. 01881
1	MS0889	J. Matthew Lane	Org. 01864
1	MS0751	Hongkyu Yoon	Org. 08864

1	MS0899	Technical Library	Org. 9536 (electronic copy)

LDRD Reports:

1	MS0359	D. Chavez, LDRD Office	Org. 1911

Sandia National Laboratories